Journal of the Korean Chemical Society
2011, *Vol. 55, No. 2*
Printed in the Republic of Korea
DOI 10.5012/jkcs.2011.55.2.268

알루미늄 부식에 대한 베타-차단제 억제제 효과

A. S. Fouda*, G. Y. El-Ewady and K. Shalabi
Department of Chemistry, Faculty of Science, El-Mansoura University, El-Mansoura - 35516, EGYPT
(접수 2010. 11. 15; 수정 2011. 1. 2; 게재확정 2011. 1. 13)

Effect of β-Blocker Inhibitors on Aluminum Corrosion

A. S. Fouda*, G. Y. El-Ewady and K. Shalabi
Department of Chemistry, Faculty of Science, El-Mansoura University, El-Mansoura - 35516, EGYPT.
**E-mail: asfouda@mans.edu.eg*
(Received November 15, 2010; Revised January 2, 2011; Accepted January 13, 2011)

요 약. 베타 차단제 억제제(atenolol, propranolol, timolol and nadolol)의 존재와 부존 하에서 0.1 M HCl 용액에 담긴 알루미늄의 부식작용을 연구하였다. 이 연구에 무게감량, 변전위 편극, 전기화학 임피던스 분석법이 사용되었다. 억제 효과는 억제제의 농도 증가에 따라 증가하였으며, 온도가 증가함에 따라 감소하였다. 모든 억제제들은 Frumkin 등온을 따르는 알루미늄 표면에 흡착되었다. 부식반응은 전하이동과정에 의해 조절됨을 발견하였다. 억제 효과 측정을 위해 사용된 실험방법 들에 대해 조사한 결과 모두 억제효과가 우수하였다.
주제어: 알루미늄, 억제, 부식, 베타-차단제 약품, 염산

ABSTRACT. Corrosion of aluminum in 0.1 M HCl solution in the absence and presence of β-blocker inhibitors (atenolol, propranolol, timolol and nadolol) was investigated using weight loss, potentiodynamic polarization and electrochemical impedance spectroscopy (EIS) techniques. The inhibition efficiency increased with inhibitor concentration and decreased with rise of temperature. Potentiodynamic polarization curves revealed that they acted as cathodic inhibitors. Some thermodynamic parameters were calculated and discussed. All inhibitors were adsorbed on Al surface obeying Frumkin isotherm. All EIS tests exhibited one capacitive loop which indicates that the corrosion reaction is controlled by charge transfer process. The inhibition efficiencies of all test methods were in good agreement.
Keywords: Aluminum, inhibition corrosion, β-blocker drugs, HCl

INTRODUCTION

Aluminum and its alloys are widely used in many industries such as reaction vessels, pipes, machineries and chemical batteries because of their advantages. They have excellent durability and corrosion resistance, but, like most materials, their behavior can be influenced by the way in which they are used. HCl solutions are used for pickling, chemical and electrochemical etching of aluminum. It is very important to add inhibitors to decrease the corrosion rate of aluminum in such solutions. Numerous organic substances containing polar functions with nitrogen, oxygen, and/or sulphur atoms in a conjucated system have been reported to exhibit good inhibiting properties.[1-5] Aliphatic and aromatic amines as well as nitrogen heterocyclic compounds were studied as corrosion inhibitors for dissolution of Al in acidic media.[6-14] Generally, it has been assumed that the first stage in the action mechanism of the inhibitors in aggressive acid media is the adsorption of the inhibitors onto the metal surface. The processes of adsorption of inhibitors are influenced by: i- the nature and surface charge of the metal ii- the chemical structure of organic inhibitors iii- the distribution of charge in the molecule iv- the type of aggressive electrolyte and iiv- the type of interaction between organic molecules and the metal surface.

The objective of the present investigation is just to investigate the effect of the investigated drugs on the corrosion behavior of aluminum in HCl solution. These inhibitors are nontoxic, relatively cheap and easy to produce in purities with proportion of more than 99% and they are rich in donating atoms such as N-, O- and S- atoms.

EXPERIMENTAL

Materials

The chemical composition of aluminum species (weight

%) is: 0.10 Si, 0.25 Fe, 0.047 Mn, 0.007 Mg, 0.002 Ni, 0.008 Cr, 0.003 Zn, 0.012 Ga, 0.001 Na, 0.007 V, 0.001 Zr, 0.007 Ti and balance Al.

Inhibitors

The following four β-blocker drugs (atenolol, propranolol, timolol and nadolol) were kindly provided from Misr Pharmaceuticals and Chemical Industries Company, Egypt and were used as received without further purification.

Solutions

Stock solutions (10^{-3} M) of these drugs were prepared by dissolving the appropriate weight of each drug separately in bidistilled water in 100 ml measuring flask. The aggressive solutions (HCl) were made of analytical reagent grade 37%. Stock solution of the acid (2 M) was prepared using bidistilled water and this concentration was checked using standard solution of Na_2CO_3.

Corrosion rate measurement

Chemical technique (Weight loss method): Aluminum sheets were cut into 2×2×0.1 cm. They were mechanically polished with emery paper (a coarse paper was used initially and then progressive fine grades were employed). They were ultrasonically degreased in alkaline degreasing mixture (15 grams Na_2CO_3 + 15 grams Na_3PO_4 per liter)[15] washed with bidistilled water and finally dried between filter papers and also weighed. Previously weighed aluminum samples were each suspended in a 100 ml beaker containing the test solution with and without the inhibitors for duration of 24 hours, with the help of glass rods and glass hooks. After the test, the samples were removed, washed with bidistilled water, dried as before and weighed again using an analytical balance (precision ± 0.1 mg). Experiments were carried out in triplicate and the data reported here represents the average value of the three tests. The weight loss of the metal in the corrosive solution is given by:

$$\Delta W = W_1 - W_2 \quad (1)$$

where W_1 and W_2 are the weights of the metal before and after exposure to the corrosive solution, respectively. The percentage inhibition efficiency (% IE) and the degree of surface coverage (θ) of the investigated compounds were calculated from equations:[16]

$$\% IE = [1 - (\Delta W_{inh} / \Delta W_{free})] \times 100 \quad (2)$$

$$\theta = [1 - (\Delta W_{inh} / \Delta W_{free})] \quad (3)$$

where ΔW_{free} and ΔW_{inh} are the weight losses of metal per unit area in the absence and presence of inhibitor at given time period and temperature, respectively.

Electrochemical techniques [potentiodynamic polarization and electrochemical impedance spectroscopy (EIS) techniques]: The working electrode was prepared from aluminum rod, inserted in a Teflon tube and isolated with Araldite so that a circular cross-section (0.785 cm^2) only was exposed. Prior to every experiment, the electrode was polished with successive different grades of emery paper, degreased with alkaline solution and rinsed by bidistilled water.

Measurements were carried out in a three-compartment electrochemical cell. The counter electrode was a platinum sheet of large surface area. The reference electrode was a saturated calomel electrode (SCE) to which all potentials are referred. The SCE was connected to the main compartment via a Luggin capillary. The cell was water-jacketed and was connected to an ultra thermostat at 25 °C. The electrode potential was allowed to stabilize for 60 mins before starting the measurements. For potentiodynamic polarization measurements the corrosion current density (j_{corr}) was determined as being a measure of corrosion rate. Stern-Geary method[17] used for the determination of corrosion current was performed by extrapolation of anodic and cathodic Tafel lines. Then j_{corr} has been used for calculation of inhibition efficiency and surface coverage (θ) as follows:[18]

$$\% IE = [1 - (j_{corr(inh)} / j_{corr(free)})] \times 100 \quad (4)$$

$$\theta = [1 - (j_{corr(inh)} / j_{corr(free)})] \quad (5)$$

where $j_{corr(free)}$ and $j_{corr(inh)}$ are the corrosion current densities in the absence and presence of inhibitor, respectively.

The potentiodynamic current-potential curves were recorded by changing the electrode potential automatically from -1500 to 500 mV with scanning rate 5 mVs^{-1}. All measurements were conducted using an electrochemical measurement system (VoltaLab 21) comprised of a PGZ 100 potentiostat, a PC and Voltamaster 4 version 7.08 software for calculations. All the experiments were carried out at 25±1°C by using ultracirculating thermostat and solutions were not deaerated to make the conditions identcial to weight loss measurements. The procedure adopted for the polarization measurements was the same as described elsewhere.[19] Each polarization was run three times and corrosion potentials and corrosion currents were reproducible within ± 5 mV and ± 1 μA cm^{-2}, respectively.

The AC impedance measurements were carried out in the frequency range 10^5-5×10^{-1} Hz with amplitude 10 mV

peak-to-peak using ac signals at the open potential circuit. All measurements were carried out using potentiostat/galvanostat Gamry PCI 300/4 connected to computer. A corrosion software model EIS 300 was employed. The experimental impedance was analyzed and interpreted on the basis of the equivalent circuit.

All chemicals were of analytical grade. The measurements were performed in 0.1 M HCl with or without the investigated β-blocker drugs in the concentration range (2×10^{-6} to 12×10^{-6} M).

The names and molecular structures of the investigated β-blocker drugs are:

Compound	Name	Structure	Molecular
(1) Atenolol	2-(4-(2-hydroxy-3-(isopropylamino) propoxy)phenyl)acetamide	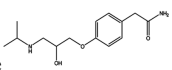	266.34
(2) Propranolol	1-(isopropylamino)-3-(naphthalen-1-yloxy)propan-2-ol hydrochloride	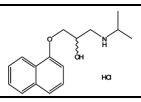	295.80
(3) Timolol	1-(tert-butylamino)-3-(4-morpholino-1,2,5-thiadiazol-3-yloxy)propan-2-ol maleate	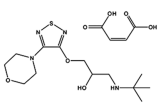	432.49
(4) Nadolol	(2R,3S)-5-(3-(tert-butylamino)-2 hydroxy propoxy) -1,2,3,4-tetrahydronaphthalene-2,3-diol	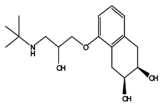	309.40

RESULTS AND DISCUSSION

Weight loss measurements

Fig. 1 showed the weight loss-time curves for the corrosion of aluminum in 0.1 M HCl in the absence and presence of different concentrations of atenolol at 25±1 °C. Curves for the other compounds were similar (not shown). According to this figure, by increasing the concentration of atenolol, the weight loss of aluminum samples will be decreased. This means that the presence of atenolol retards the corrosion of aluminum in HCl or in other words, atenolol acts as inhibitor. The linear variation of weight loss with time in uninhibited and inhibited acid indicated the absence of insoluble surface films during corrosion.

Obtained values of % IE were given in *Table* 1, the order of inhibition efficiency of the investigated compounds is as follows: atenolol > propranolol > timolol > nadolol.

Adsorption isotherm

The nature of inhibitor interaction on the corroding surface during corrosion inhibition of metals and alloys has been deduced in terms of adsorption characteristics on the inhibitor.[20] The surface coverage (θ) data are very useful

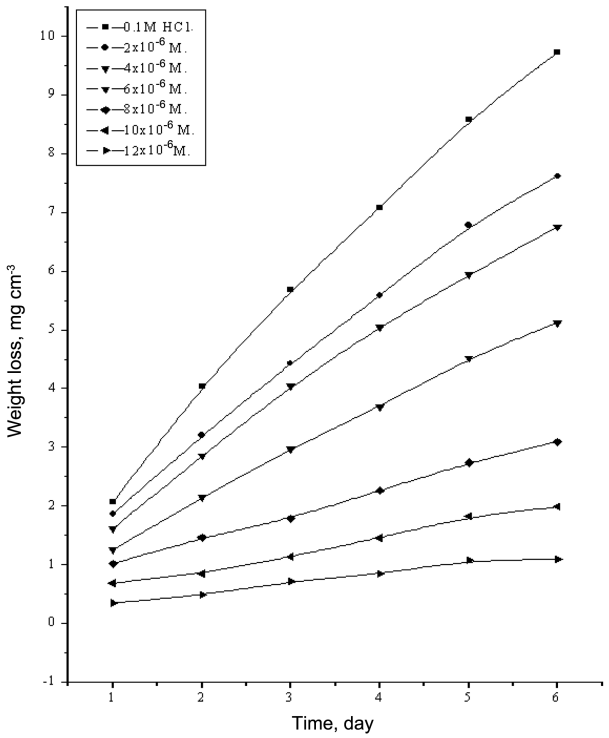

***Fig.* 1.** Weight loss-time curves for the corrosion of aluminum in 0.1 M HCl in the absence and presence of different concentrations of atenolol at 25 °C.

***Table* 1.** % Inhibition efficiency at different concentrations of the investigated drugs for the corrosion of aluminum in 0.1 M HCl at 25 °C

Concentration/ M	% IE			
	atenolol	propranolol	timolol	nadolol
2×10^{-6}	21.3	15.9	15.8	9.9
4×10^{-6}	28.6	28.1	26.8	25.0
6×10^{-6}	47.8	40.9	39.4	38.2
8×10^{-6}	68.0	63.8	56.2	51.2
10×10^{-6}	79.4	72.3	69.5	66.3
12×10^{-6}	88.2	81.9	78.1	72.9

when discussing the adsorption characteristics. Assuming no change in the mechanism of hydrogen evolution reaction (HER) and aluminum dissolution, the surface coverage of each inhibitor at a given concentration can be calculated from equations 3 & 5. The plot of θ vs.log C for all investigated compounds gave an S-type curve (*Fig.* 2) characteristic of the Frumkin adsorption isotherm[21] as given by:

$$(\theta/1-\theta)\exp(-f\theta) = K_aC \quad (6)$$

where K_a is the equilibrium constant of adsorption and f is another constant. The constant K_a is related to the standard

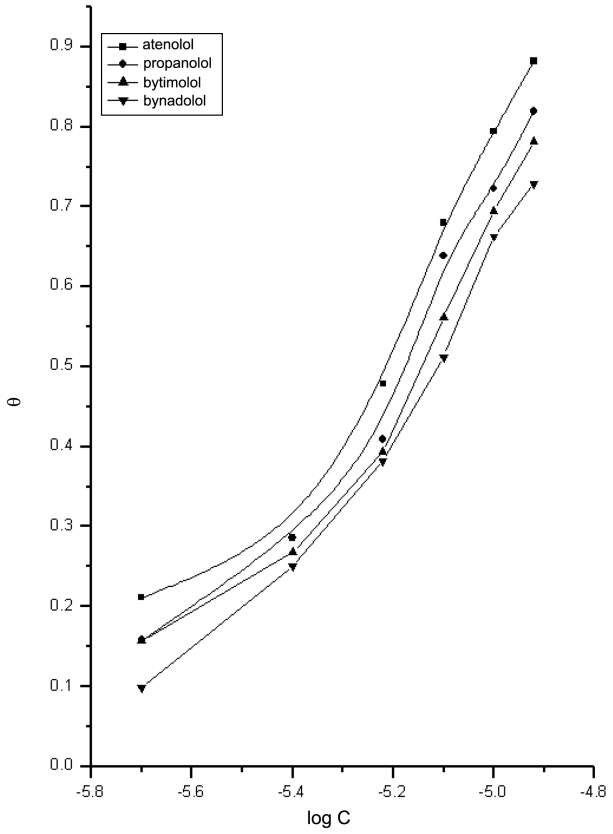

***Fig.* 2.** θ vs. log C for corrosion of aluminum in 0.1 M HCl in presence of different concentrations of some β blocker compounds at 25 °C.

free energy of adsorption ΔG^{o}_{ads} by the equation:

$$K_a = 1/55.5 \exp(-\Delta G^{o}_{ads} / RT) \quad (7)$$

The value of 55.5 is the concentration of water in solution expressed in M L^{-1}.

Potentiodynamic polarization

Fig. 3 gathers the cathodic and anodic polarization curves of aluminum in free acid and in the presence of atenolol at different concentrations. Similar curves were obtained for other compounds (not shown). The collected electrochemical parameters values of corrosion potential (E_{corr}), anodic Tafel slope (β_a,), the corrosion current density (j_{corr}), the degree of surface coverage (θ) and the inhibition efficiency (% IE) are presented in *Table* 2. The data in *Table* 2 showed that the anodic Tafel slope remained almost unchanged for inhibited and uninhibited systems, indicating that the inhibitive action of these drugs was due to adsorption of these inhibitor molecules on the cathodic active sites. In this case, anodic dissolution of aluminum was suppressed without changing its mechanism. The values of (E_{corr}) were shifted to the cathodic direction by increasing the inhibitor concentration, indicating cathodic control mechanism. The value of (j_{corr}) decreases with the increase of inhibitor concentration which associated with an increase in % IE.

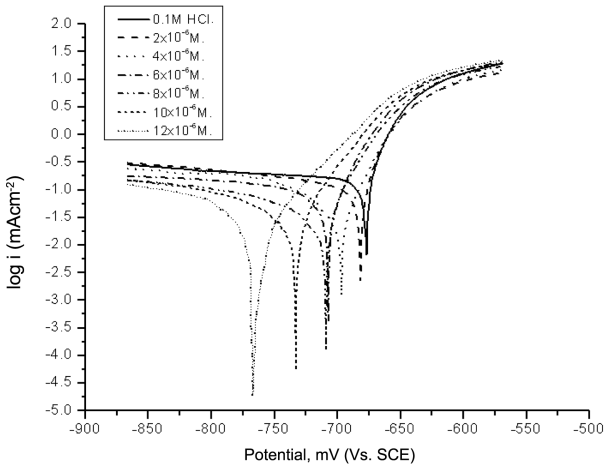

***Fig.* 3.** Potentiodynamic polarization curves for the corrosion of aluminum in 0.1 M HCl in the absence and presence of different concentrations of atenolol at 25 °C.

These results showed that the inhibition efficiency of these inhibitors was depending on the electrode potential; then, the tested compounds were acting predominantly as cathodic inhibitors. The limitation of inhibitory action on cathodic domain is found by different researchers.[22-25] In this case, the inhibition is generally interpreted by the formation of a protective layer of adsorbed inhibitor species at the electrode surface.[26]

The order of inhibition efficiency of the investigated compounds is as follows: atenolol > propranolol > timolol > nadolol. This is also in agreement with the observed order of corrosion inhibition by the weight loss method.

Effect of temperature and activation parameters of inhibition process

The influence of temperature on the corrosion rate of aluminum in 0.1 M HCl in the absence and presence of 2×10^{-6} M of the investigated compounds was investigated by the potentiodynamic polarization technique in temperature range (30-60 °C).

The dependence of corrosion current density on the temperature can be expressed by Arrhenuis equation:

$$k = A \exp(-E_a^*/RT) \quad (8)$$

where A is the pre-exponential factor and E_a^* is the apparent activation energy of the corrosion process. Arrhenuis

***Table* 2.** The effect of concentration of the investigated compounds on the free corrosion potential (E_{corr}), corrosion current density (I_{corr}), Tafel slopes (β_a & β_c), inhibition efficiency (% IE), degree of surface coverage (θ) and corrosion rate for the corrosion of aluminum in 0.1 M HCl at 25°C

Compounds	Conc., M	E_{corr}, mV	I_{corr}, mA cm^{-2}	$-\beta_c$, mV dec^{-1}	β_a, mV dec^{-1}	θ	% IE	Corrosion rate mm/year
Free acid	0	-681.5526	0.1552	794	26	0.0000	0.00	1.6893
I	2×10^{-6}	-684.5957	0.1187	400	27	0.2355	23.55	1.2916
	4×10^{-6}	-697.4234	0.0991	313	37	0.3617	36.17	1.0783
	6×10^{-6}	-707.7521	0.0783	252	32	0.4958	49.58	0.8518
	8×10^{-6}	-712.0835	0.0431	222	32	0.7222	72.22	0.4693
	10×10^{-6}	-735.2399	0.0299	118	36	0.8076	80.76	0.3251
	12×10^{-6}	764.8934	0.0127	52	39	0.9180	91.80	0.1385
II	2×10^{-6}	-689.6713	0.1198	512	26	0.2280	22.80	1.3042
	4×10^{-6}	-697.2235	0.1076	443	26	0.3069	30.69	1.1709
	6×10^{-6}	-695.5242	0.0850	347	26	0.4521	45.21	0.9255
	8×10^{-6}	-699.4891	0.0574	282	26	0.6299	62.99	0.6252
	10×10^{-6}	-705.5309	0.0289	116	26	0.8139	81.39	0.3144
	12×10^{-6}	-713.4607	0.0153	55	26	0.9012	90.12	0.1669
III	2×10^{-6}	-684.9067	0.1250	498	26	0.1943	19.43	1.3612
	4×10^{-6}	-689.9045	0.1092	318	26	0.2964	29.64	1.1887
	6×10^{-6}	-691.1040	0.0912	268	23	0.4122	41.22	0.9930
	8×10^{-6}	-693.3030	0.0709	183	20	0.5429	54.29	0.7722
	10×10^{-6}	-694.9023	0.0464	93	22	0.7012	70.12	0.5048
	12×10^{-6}	-695.3021	0.0289	67	16	0.8138	81.38	0.3146
IV	2×10^{-6}	-686.5060	0.1283	522	22	0.1735	17.35	1.3963
	4×10^{-6}	-688.1053	0.1130	423	25	0.2716	27.16	1.2305
	6×10^{-6}	-690.3043	0.0883	187	24	0.4311	43.11	0.9611
	8×10^{-6}	-692.3034	0.0698	161	22	0.5500	55.00	0.7602
	10×10^{-6}	-695.5020	0.0508	131	19	0.6728	67.28	0.5527
	12×10^{-6}	-699.7001	0.0387	85	22	0.7505	75.05	0.4215

plot obtained for the corrosion of aluminum in HCl solution is shown in *Fig*. 5. Values of E_a were determined by regression between log k (corrosion rate) versus (1/T) and given in *Table* 3.

Values of E_a^* denote the energy barrier for the chemical reaction, and lower E_a^* values means lower energy barrier for the aluminum corrosion.[27] Enthalpy and entropy of activation (ΔH^*, ΔS^*) of the corrosion process were calculated from the transition state theory (*Table* 3):

$$\text{Rate} = RT/Nh \exp(\Delta S^*/R) \exp(-\Delta H^*/RT) \quad (9)$$

where h is Planck's constant and N is Avogadro's number. A plot of log (corrosion rate/ T) vs. 1/ T gave straight lines as shown in *Fig*. 5, for aluminum in 0.1 M HCl at 2×10^{-6} M investigated compounds. Values of ΔH^* showed the same trend as that observed in E_a^* values. The values of entropy of activation were large and negative. This implies that the activated complex represents association rather than dissociation, indicating that a decrease in disorder takes place, going from reactants to the activated complex.[28]

The order of inhibition efficiency of the investigated compounds as gathered from the increase in E_a^* and ΔH^*_{ads} values and decrease in ΔS^*_{ads} values, is as follows: atenolol > propranolol > timolol > nadolol.

Electrochemical impedance spectroscopy measurements

The influence of different concentrations of atenolol drugs on impedance spectra of aluminum in 0.1 M HCl solution at E_{oc} and at 25 °C is shown in *Fig.* 6. These were analyzed by fitting the experimental data to a simple equivalent circuit model shown below, which includes the solution resistance R_s and the double layer capacitance C_{dl} which is placed in parallel to the charge transfer resistance R_{ct}.

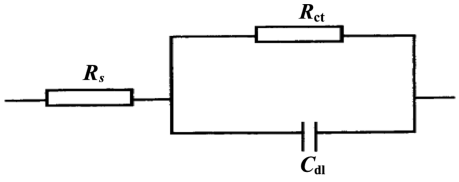

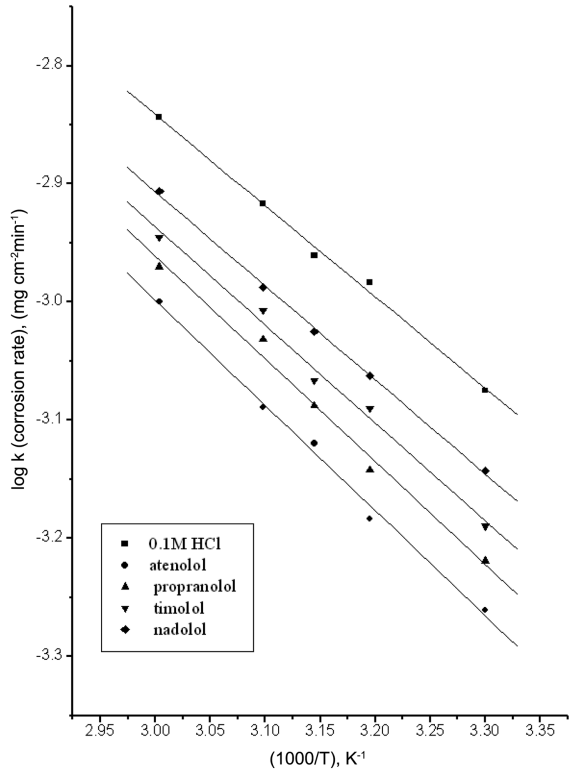

***Fig*. 4.** log corrosion rate -1/T curves for the corrosion of aluminum in 0.1 M HCl at 2×10^{-6} for the investigatyed drugs.

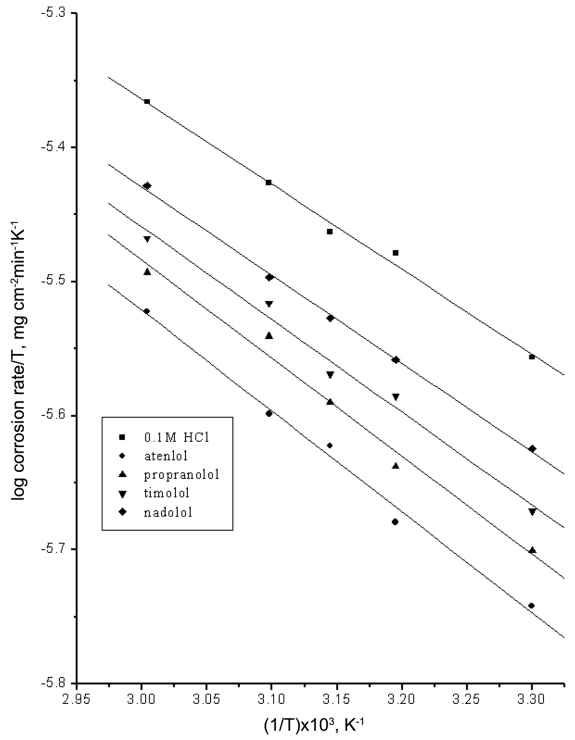

***Fig*. 5.** log (corrosion rate/T) - (1/T) curves for the corrosion of aluminum in 0.1 M HCl at 2×10^{-1} for the investigatyed drugs.

***Table* 3.** Activation parameters of the corrosion of aluminum in 0.1 M HCl at 2×10^{-6} M for the investigated drugs

Compounds	Activation parameters		
	E_a^* / J mol^{-1}	ΔH^* / kJ mol^{-1}	$-\Delta S^*$ / J mol^{-1} K^{-1}
Free acid	14.8	12.1	263.9
atenolol	17.0	14.4	260.1
propranolol	16.7	14.0	260.6
timolol	15.9	13.2	262.4
nadolol	15.3	12.6	263.7

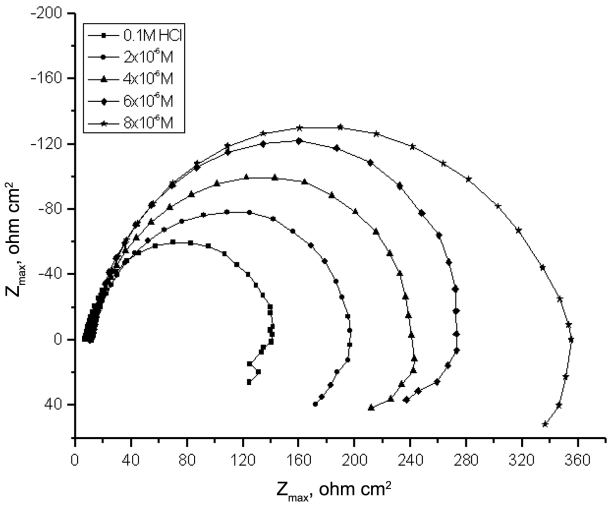

***Fig*. 6.** The Nyquist plots for aluminum in 0.1 M HCl solution in the absence and presence of different concentrations of atenolol at 25 °C.

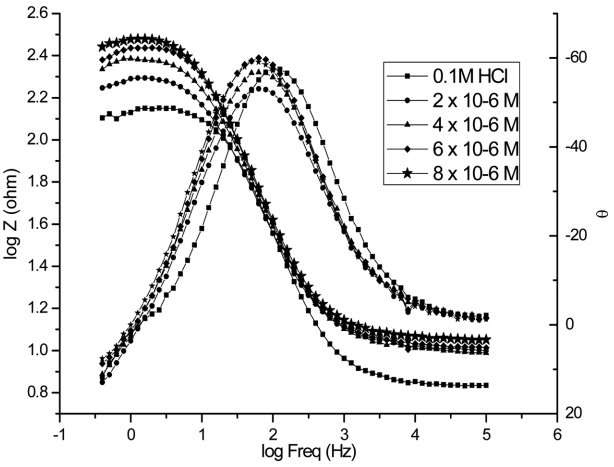

***Fig*. 7.** The Bode plots for aluminium in 0.1 M HCl solution in the absence and presence of different concentrations of atenolo at 25 °C.

Fig. 7 represents the Bode plots for atenolol. Similar curves were obtained for other compounds (not shown). The impedance parameters derived from these investigations were mentioned in *Table* 4. In most cases, the obtained Nyquist impedance diagrams do not show perfect semi-

***Table* 4.** Electrochemical kinetic parameter obtained by EIS technique for the corrosion of aluminum in 0.1 M HCl at different concentrations of investigated compounds at 25 °C

Compound	Concentration / M	C_{dl} / μF cm^{-2}	R_{ct} / Ω cm^2	θ	% / IE
Free acid	0.0	74.8	125.3	0.0000	0.0
atenolol	2×10^{-6}	52.3	167.4	0.2515	25.2
	4×10^{-6}	47.4	211.6	0.4079	40.8
	6×10^{-6}	45.8	246.3	0.4913	49.1
	8×10^{-6}	43.7	346.49	0.6384	63.8
propranolol	2×10^{-6}	62.4	165.8	0.2443	24.4
	4×10^{-6}	59.6	201.1	0.3769	37.7
	6×10^{-6}	44.8	218.9	0.4276	42.8
	8×10^{-6}	41.3	325.6	0.6152	61.5
timolol	2×10^{-6}	61.3	154.2	0.1874	18.7
	4×10^{-6}	49.9	179.9	0.3035	30.4
	6×10^{-6}	45.7	213.2	0.4123	41.2
	$8x10^{-6}$	34.5	289.4	0.5670	56.7
nadolol	2×10^{-6}	56.5	150.7	0.1686	16.9
	4×10^{-6}	54.7	166.2	0.2461	24.6
	6×10^{-6}	52.1	211.8	0.4084	40.8
	8×10^{-6}	47.8	273.8	0.5424	54.2

circle, generally attributed to the frequency dispersion[29] of interfacial impedance. This anomalous phenomenon is interpreted by the inhomogeneity arising from surface roughness or interfacial phenomena.[30,31] As the obtained impedance diagram has a semicircle appearance, it showed that the corrosion of aluminum is mainly controlled by a charge transfer process. The data revealed that, each impedance diagram consists of a large capacitive loop with low frequency dispersion (inductive arc). This inductive arc is generally attributed to anodic adsorbed intermediates controlling the anodic process.[32-35] To follow this, inductive arc will be disregarded. The impedance diagrams in absence and presence of different concentrations of inhibitors, showed the same trend (one capacitive loop); however, the diameter of this capacitive loop increased with increasing concentration. In addition to the high frequency capacitive loop, the semicircles were rolled over and extended to the fourth quadrant, and the pseudo-inductive loop at low frequency end was observed, indicating that Faradic process is taking place on the free electrode sites. This inductive loop is generally attributed to the adsorption of species resulting from the aluminum dissolution and the adsorption of hydrogen.[36] The main parameters deduced from the analysis of Nyquist diagrams were the charge transfer resistance (R_{ct}). These parameters were calculated from the difference in impedance at lower and higher frequencies, the double layer capacitance (C_{dl}) and the frequency at which the imaginary component of the impedance is maximal ($-Z_{max}$) were found as presented in equation:

$$C_{dl} = \frac{1}{2\pi f_{max} R_{ct}} \quad (10)$$

In fact, the presence of the investigated drugs led to decreasing the values of C_{dl} due to the decrease of the local dielectric constant and/or from the increase of thickness of the electrical double layer.[37] It was suggested that the inhibitor molecules were functioned by adsorption at the metal / solution interface. Thus, the decrease in C_{dl} values and the increase in R_{ct} values and consequently, the inhibition efficiency may be reported as the gradual replacement of water molecules (volumes of the water molecules is 27.2 A^3) by the adsorption of the inhibitor molecules from the metal surface, and by decreasing the extent of dissolution reaction. In the Bode plot the high frequency limits corresponded to the solution resistance R_s. The low frequency limit referred to the sum of R_s and R_{ct}, which is generally determined by both the electronic or ionic conductivity of the surface film and polarization resistance. The phase angle against log f plot showed the phase angle dropping zero at high and low frequencies, corresponding to the resistive behavior of R_s and (R_s + R_{ct}).

The inhibition efficiency and the surface coverage (θ) obtained from the impedance measurements were defined by the following relations:

$$\% IE = [1 - (R^o_{ct} / R_{ct}] \times 100 \quad (11)$$

$$\theta = [1 - (R^o_{ct} / R_{ct})] \quad (12)$$

where R^{o}_{ct} and R_{ct} are the charge transfer resistance in the absence and presence of inhibitor, respectively. The % IE obtained from EIS measurements were close to those deduced from polarization and weight loss methods. The order of inhibition efficiency obtained from EIS measurements is as follows: atenolol > propranolol > timolol > nadolol.

Mechanism of corrosion inhibition with these drugs

By knowing this mechanism of aluminum dissolution in HCl, the adsorption mechanism of investigated drugs on positive charged Al surface can be predicted. The mechanism of anodic dissolution of Al follows the following steps:

$$Al + Cl^{-} \leftrightarrow AlCl^{-}_{ads} \quad (13a)$$

The cathodic hydrogen evolution reaction follows the following steps:

$$H^{+} + e \rightarrow H_{ads} \text{ (fast)} \quad (13b)$$
$$H^{+} + H_{ads} + e \rightarrow H_2 \quad (13c)$$

The cationic form of investigated drugs can interact with $AlCl^{-}_{ads}$ species formed in step (13a). The cationic form of investigated drugs can also be adsorbed on the cathodic sites of Al in competition with the hydrogen ions (step 13c), also, these compounds may be adsorbed on Al surface via the negatively charged centers in the molecules and via the π bonds of the aromatic systems of the positively charged Al surface. This enhances the % IE to great extent. Similar results have been observed before.[38] Skeletal representation of the mode of adsorption of the investigated compounds on aluminum surface was shown in *Fig*. 8, According to this figure, there are only three adsorption active centers (two oxygen atoms and one N atom) in the similar part in all molecules. So the type and structure of R are the effective parts. Atenolol contains one more active centre (N atom of NH_2) and it lies flat on the aluminum surface, so, most of surface area will be covered and hence, more inhibition efficiency is observed. Propranolol has naphathayl ring which rotates around the bond of C----O and covers most of the surface area but less than atenolol. Timolol and nadolol are adsorbed on aluminum surface through the three active centers (two oxygen atoms and one N atom) and the remainder part of molecules may be lies perpendicular on aluminum surface, so a little part of the surface area will be covered and also the presence of t-methyl group in these molecules will cause a steric hindrance for the adsorption of these molecules on Al surface and hence lower inhibition efficiency was obtained, so both timolol and nadolol come after atenolol and propranolol in inhibition efficiency.

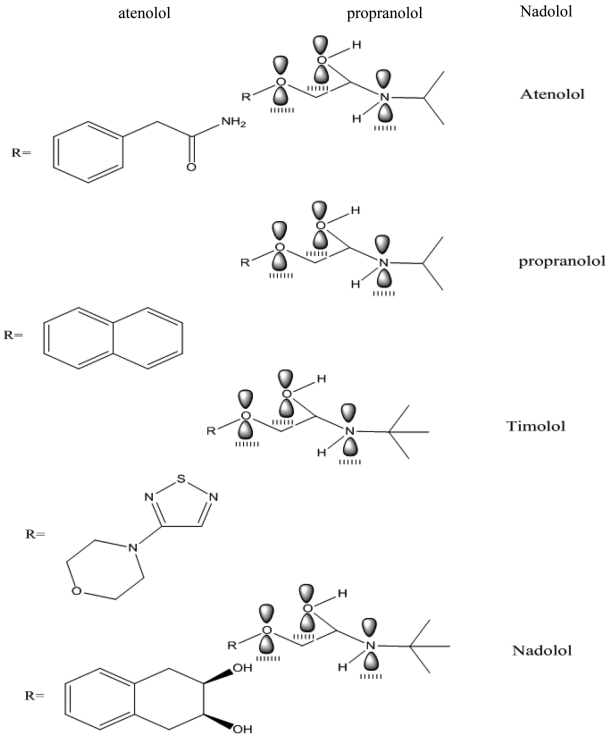

***Fig*. 8.** Skeletal representation of the mode of adsorption of the investigated compounds.

Quantum chemical parameters of investigated compounds

The E_{HOMO} indicates the ability of the molecule to donate electrons to an appropriated acceptor with empty molecular orbital and E_{LUMO} indicates its ability to accept electrons. The lower the value of E_{LUMO}, the more ability of the molecule is to accept electrons.[39] While, the higher is the value of E_{HOMO} of the inhibitor, the easer is its offering electrons to the unoccupied d-orbital of metal surface and the greater is its inhibition efficiency. The calculations listed in *Table* 5 showed that the highest energy E_{HOMO} is assigned for the atenolol, which is expected to have the highest corrosion inhibition among the investigated compounds. The presence of methoxy group stabilizes the HOMO level which is most observed in the case of atenolol *Table* 5. Therefore, it has the greatest tendency to adsorb on the metal surface and accordingly has the highest inhibition efficiency. This expectation is in a good agreement with the experimental observations suggesting the highest inhibition efficiency for atenolol among the other investigated inhibitors *Table* 5. The propranolol has lower E_{HOMO} value than that of atenolol which is probably

***Table* 5.** The calculated quantum chemical parameters for investigated compounds

parameter	atenolol	propranolol	nadolol
E_{HOMO} (eV)	-9.473	-9.081	-9.623
E_{LUMO} (eV)	-0.134	-0.827	-0.116
ΔE (eV)	9.339	8.254	9.507
μ (debyes)	5.093	1.630	5.263
η (eV)	4.669	4.127	4.754
σ (eV^{-1})	0.214	0.242	0.210
Pi (eV)	-4.8035	-4.954	-4.8695
χ (eV)	4.8035	4.954	4.8695

due to the effect of Cl group. So, it is expected that -OCH_3 containing compounds have higher inhibition efficiency than -Cl and -COOH containing compounds. Furthermore, the HOMO level is mostly localized on the two benzene moiety, imino and hydroxyl groups indicating that the preferred sites for electrophilic attack at the metal surface are through the nitrogen and oxygen atoms (*Fig*. 9). This means that the two benzene moiety with high coefficients of HOMO density was oriented toward the metal surface and the adsorption is probably occurred through the p-electrons of the two benzene moiety and the lone pair of nitrogen and oxygen. It was found that the variation of the calculated LUMO energies among all investigated inhibitors is rule lessly, and the inhibition efficiency is misrelated to the changes of the E_{LUMO} (*Table* 5). The HOMO-LUMO energy gap, ΔE approach, which is an important stability index, is applied to develop theoretical models for explaining the structure and conformation barriers in many molecular systems. The smaller is the value of ΔE, the more is the probable inhibition efficiency that the compound has.[40-42] The dipole moment μ, electric field, was used to discuss and rationalize the structure.[43] It was shown from *Table* 5 that atenolol molecule has the smallest HOMO-LUMO gap compared with the other molecules. Accordingly, it could be expected that atenolol molecule has more inclination to adsorb on the metal surface than the other molecules. The higher is the value of μ, the more is the probable inhibition efficiency that the compound has. The calculations showed that the highest value of μ is assigned for the atenolol which has the highest inhibition efficiency. Absolute hardness h and softness σ are important properties to measure the molecular stability and reac-

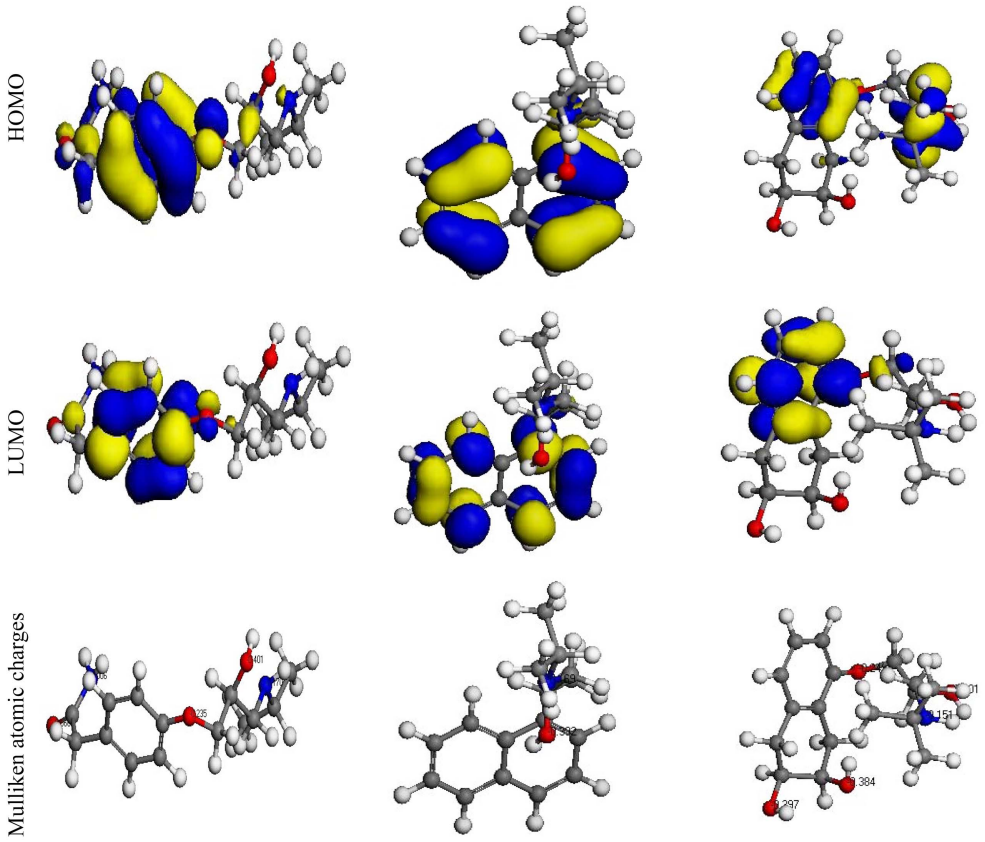

***Fig*. 9.** The optimized molecular structures, HOMO, LUMO and Mulliken atomic charges of the inhibitor molecules using PM3.

tivity. A hard molecule has a large energy gap and a soft molecule has a small energy gap. Soft molecules are more reactive than hard ones because they could easily offer electrons to an acceptor. For the simplest transfer of electrons, adsorption could occur at the part of the molecule where σ, which is a local property, has the highest value.[44] In a corrosion system, the inhibitor acts as a Lewis base while the metal acts as a Lewis acid. Bulk metals are soft acids and thus soft base inhibitors are most effective for acidic corrosion of those metals. Accordingly, it is concluded that inhibitor with the highest σ value has the highest inhibition efficiency (*Table* 5) which is in a good agreement with the experimental data.

This is also confirmed from the calculated inhibition efficiencies of molecules as a function of the inhibitor chemical potential, Pi, and the fraction of charge transfer, ΔN to the metal surface. The relatively good agreement of Pi and ΔN with the inhibition efficiency could be related to the fact that any factor causing an increase in chemical potential would enhance the electronic releasing power of inhibitor molecule (*Table* 5).

It was noteworthy that the presence of an electron donating substituent such as -OCH_3 group is more favored than -Cl or -COOH group to increase the inhibition efficiency of the inhibitor. The use of Mulliken population analysis to estimate the adsorption centers of inhibitors has been widely reported and it is mostly used for the calculation of the charge distribution over the whole skeleton of the molecule.[45]

There is a general consensus by several authors that the more negatively charged heteroatom is, the more is its ability to adsorb on the metal surface through a donor-acceptor type reaction.[46-48]

Variation in the inhibition efficiency of the inhibitors depends on the presence of electronegative O- and N-atoms as substituents in their molecular structure. The calculated Milliken charges of selected atoms are presented in *Fig*. 9.

CONCLUSIONS

β-blocker drugs show good corrosion inhibition property against aluminum corrosion in acidic media. Inhibition efficiencies are related to concentration, temperature and chemical structure of the β-blockers. Results of polarization showed that these β-blockers are cathodic inhibitors. Adsorption of these β-blockers on aluminum surface obeys Frumkin adsorption isotherm. The results obtained from weight loss, polarization curves and impedance methods are in good agreement.

REFERENCES

1. Abdallah, M. *Corros. Sci.* **2004**, *46*, 1981.
2. Maayta, A. K.; Al-Rawashdeh, N. A. F. *Corros. Sci.* **2004**, *46*, 1129.
3. Oguzie, E. E. *Mater. Lett.* **2005**, *59*, 1076.
4. Popova, A.; Christov, M.; Raicheva, S.; Sokolova, E. *Corros. Sci.* **2004**, *46*, 1333.
5. Gomma, G. K. *Mater. Chem. Phys.* **1998**, *55*, 243.
6. Granese, S. L. *Corrosion* **1988**, *44*, 322.
7. Mimani, T.; Mayanna, S. M.; Munichandraiah, N. *J. Appl. Electrochem.* **1993**, *23*, 339.
8. Schmitt, G.; Bedlur, K. *Werkst. Korros.* **1985**, *36*, 273.
9. Hukovic, M. A.; Grubac, Z.; Lisac, E. S. *Corrosion* **1994**, *50*(2), 146.
10. Mahmoud, S. S.; El-Mahdy, G. A. *Corrosion* **1997**, *53*(6), 437.
11. Fouda, A. S.; Moussa, M. N.; Taha F. I.; Elneanaa, A. I. *Corros. Sci.* **1986**, *26*, 719.
12. Fouda, A. S.; Al-Sarawy, A. A.; Ahmed F. S.; El-Abbasy, H. M., *Corros. Sci.* **2009**, *51*, 485.
13. Noor, E. N. *Mater. Chem. Phys.* **2009**, *114*, 533
14. Obot, L. B.; Obi-Egbedi, N. O.; Umoren, S. A. *Corros. Sci.* **2009**, *51*, 276.
15. Maayta, A. K.; Rawshdeh, N. A. F. *Corros. Sci.* **2004**, *46*, 1129.
16. Derya Lece, H.; Emregul, K. C.; Atakol, O. *Corros. Sci.* **2008**, *50*, 1460.
17. Stern, M.; Geary, A. I. J. *J. Electrochem. Soc.* **1957**, *104*, 56.
18. Bentiss, F.; Jama, C.; Mernari, B.; El Attari, H.; El Kadi, L.; Lebrini, M.; Traisnel, M.; Lagrenee, M. *Corros. Sci.* **2009**, *51*, 1628.
19. Bentiss, F.; Lagrenee, M.; Traisnel, M.; Hornez, J. C. *Corros. Sci.* **1999**, *41*, 789.
20. Dinnappa, R. K.; Mayanna, S. M. *J. Appl. Elcreochem.* **1982**, *11*, 111.
21. Frumkin, A. N. *Z. Phys. Chem.* **1925**, *116*, 466.
22. Mengoli, G.; Musiani, M. M.; Pagura, C.; Paoulucci, F. *Corros. Sci.* **1991**, *32*, 743.
23. Elkholy, A.; Etman, M.; Kertit, S.; Aride, J.; Ben Bachir A.; Srhiri, A. *J. Appl. Electrochem.* **1989**, *9*, 512.
24. Aksut, A. A.; Lorenz, W. J. L.; Mansfeld, F. *Corros. Sci.* **1982**, *22*, 611.
25. Lorenz, W. J.; Mansfeld, F. *Corros. Sci.* **1981**, *21*, 647.
26. Lorenz, W. J.; Mansfeld, F. *Corros. Sci.* **1986**, *31*, 467.
27. Tang, L.; Li, X.; Li, L.; Mu, G.; Liu, G. *mater. Chem. Phys.* **2006**, *97*, 301
28. Fouda, A. S.; Al-Sarawy, A. A.; El-Katori, E. E. *Desalination*. **2006**, *201*, 1.
29. Bentiss, F.; Lebrini, M.; lagrenee, M. *Corros. Sci.* **2005**, *47*, 2915.
30. Shih, H.; Mansfeld, H. *Corros. Sci.* **1989**, *29*, 1235.
31. Martinez, S., Metikos-Hukovic, M. *J. Appl. Electrochem.* **2003**, *33*, 1137.

32. Paskossy, T., *J. Electroanal. Chem.* **1994**, *364*, 111.
33. Caprani, A.; Epelboin, I.; Morel, Ph.; Takenouti H. *proceedings of the 4th European sym. on Corros. Inhibitors*: Ferrara, Italy, **1975**, 571.
34. Bessone, J.; Mayer, C.; Tuttner, K.; lorenz, W. *J. Electrochim. Acta* **1983**, *28*, 171.
35. Epelboin, I.; Keddam, M.; Takenouti, H. *J. Appl. Electrochem.* **1972**, *2*, 71.
36. Lebrini, M.; Lagrenee, M.; Vezin, H.; Gengembre, L.; Bentiss, F. *Corros. Sci.* **2005**, *47*, 485.
37. McCafferty, E.; Hackerman, N. *J. Electrochem. Soc.* **1972**, *119*, 146.
38. Yurt, A.; Ulutas, S.; Dal, H. *Appl. Surf. Sci.* **2006**, *253*, 919.
39. Zhang, D. Q.; Gao, L. W.; Zhou, G. D. *Corros. Sci.* **2004**, *46*, 3031.
40. Gao, G.; Liang, C.; *Electrochim. Acta* **2007**, *52*, 4554.
41. Feng, Y.; Chen, S.; Guo, Q.; Zhang, Y.; Liu, G. *J. Electroanal. Chem.* **2007**, *602*, 115.
42. Gece, G.; Bilgic, S. *Corros. Sci.* **2009**, *51*, 1876.
43. Martýnez, S., *Mater. Chem. Phys.* **2002**, *77*, 97.
44. Ozcan, M.; Dehri, I.; Erbil, M.; *Appl. Surf. Sci.* **2004**, *236*, 155.
45. Roque, J.M.; Pandiyan, T.; Cruz, J.; Garclá-Ochoa, E. *Corros. Sci.* **2008**, *50*, 614.
46. Kandemirli, F.; Sagdinc, S. *Corros. Sci.* **2007**, *49*, 2118.
47. Bereket, G.; Ogretic, C.; Ozsahim, C. *J. Mol. Struct. (THEOCHEM)* **2003**, *663*, 39.
48. Li, W.; He, Q.; Pei, C.; Hou, *B. Electrochim. Acta*. **2007**, *52*, 6386.